

Supplemental materials

Heterogeneous UV Disinfection Aided by ZnO/Al₂O₃ Composites for Inhibiting Antibiotic Resistant Bacteria Photoreactivation and Gene Recovery

Xu Wang ^{a, b}, Baiyu Zhang ^d, Hua Ren ^e, Yibin Jia ^{a, b}, Honghuan Xia ^{a, b},
Ping Guo ^{a, b, c*}

^a Key Lab of Groundwater Resources and Environment, Ministry of Education, Jilin University, Changchun 130021, People's Republic of China

^b College of New Energy and Environment, Jilin University, Changchun 130021, People's Republic of China

^c State Key Laboratory of Superhard Materials, Jilin University, Changchun 130021, People's Republic of China

^d Department of Civil Engineering, Faculty of Engineering and Applied Science, Memorial University, St. John's, NL, Canada A1B 3X5

^e Department of Ophthalmology, The First Hospital of Jilin University, Changchun, China

*E-mail: guoping@jlu.edu.cn

Text S1 Preparation and characterization of synthesized ZnO@Al₂O₃ particles

1. Preparation processes

Two steps for synthesizing ZnO@Al₂O₃ were required in this paper, i.e. preparation of Al₂O₃ particles by template method then loading ZnO on Al₂O₃ via solvothermal method. Firstly, 16 g epoxy resin, 18 g polyethylene glycol 1000 and 14 g polyethylene glycol 2000 were melt down and stirred, then immediately added 4 g diethylenetriamine. Before the mixed solution began to solidify, poured the mixture into a polytetrafluoroethylene container to age under 70 °C. After 3 h aging, the white organic template was dried under 25 °C for one day. 100 mL 56.25 g/L Al(NO₃)₃ solution was slowly dropped into 100 mL 0.5% chitosan/acetic acid, and 5 g template pieces (1 cm × 1 cm × 1 cm) were mixed together. Ammonia was dropped into the mixtures after 1 h stirring until emulsible colloidal substances occurred and pH reached around 8.5. The colloidal substances were collected through 0.45 μm filter after aging 1 h under 70 °C, then cleaned the collection with distilled water three times and dried it under 80 °C for one day. The air-dried substances were calcinated under 500 °C for 6 h. After thoroughly pulverization, the Al₂O₃ particles were gained.

The mixtures of 3.655 g Zn(NO₃)₂ · 6H₂O and 1.646 g Na₂C₂O₄ were grinded for 10 min then were washed out with distilled water at 5000 rpm centrifugation until the conductivity of supernatant below 20 μS/cm. 0.116g dried precipitation, 0.5 g Al₂O₃ particle and 30 mL distilled water in polytetrafluoroethylene hydrothermal reactor were reacted under 200 °C for 6 h. ZnO@Al₂O₃ particle was gained after cleaning, drying and grinding.

2. Characterizations

Pure Al₂O₃ and ZnO particles have been already characterized in previous researches (Le et al., 2020; Lei et al., 2013; Martin et al., 1995; Yao et al., 2013), and we did not repeat these actions in our study.

Band gap energy could be gained by Eq. S1:

$$E_g = \frac{hc}{\lambda} \quad \text{Eq. S1}$$

where E_g was band gap energy; h was the Planck's constant ($h=4.135667 \times 10^{-15} \text{ eV}\cdot\text{s}$); c was the light speed ($c=3 \times 10^8 \text{ m/s}$) and λ was the absorption wavelength of absorption edge.

References

- Le, A. T., Ahmadipour, M., Pung, S. Y., 2020. A review on ZnO-based piezoelectric nanogenerators: Synthesis, characterization techniques, performance enhancement and applications. *J. Alloy. Compd.*, 844, 156172.
- Lei, Z., Wu, L., Gao, L., Liu, M., Shui, H., Wang, Z., Ren, S., 2013. Synthesis, characterization and evaluation of Ni–Mo/Zr–Al₂O₃ catalyst for hydro-conversion of lignite-based heavy carbon resources. *J. Ind. Eng. Chem.*, 19(5), 1421-1425.
- Martin, C., Martin, I., Rives, V., Damyanova, S., Spojakina, A., 1995. Characterization and Fourier transform infrared spectroscopic study of surface acidity in NiMo/TiO₂-Al₂O₃ catalysts. *Spectrochim. Acta A*, 51(11), 1837-1845.
- Yao, X., Gao, F., Dong, L., 2013. The application of incorporation model in γ -Al₂O₃ supported single and dual metal oxide catalysts: A review. *Chinese J. Catal.*, 34(11), 1975-1985.

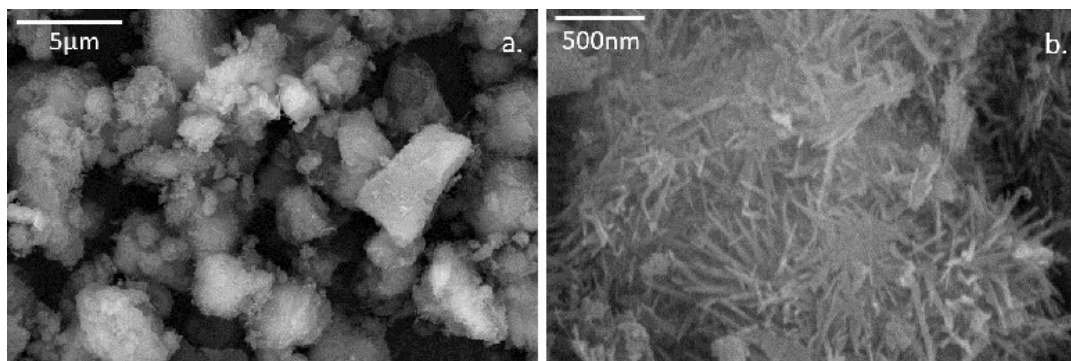


Figure S1 SEM images of ZnO@Al₂O₃ at scales of (a.) 5 μm and (b.) 500 nm

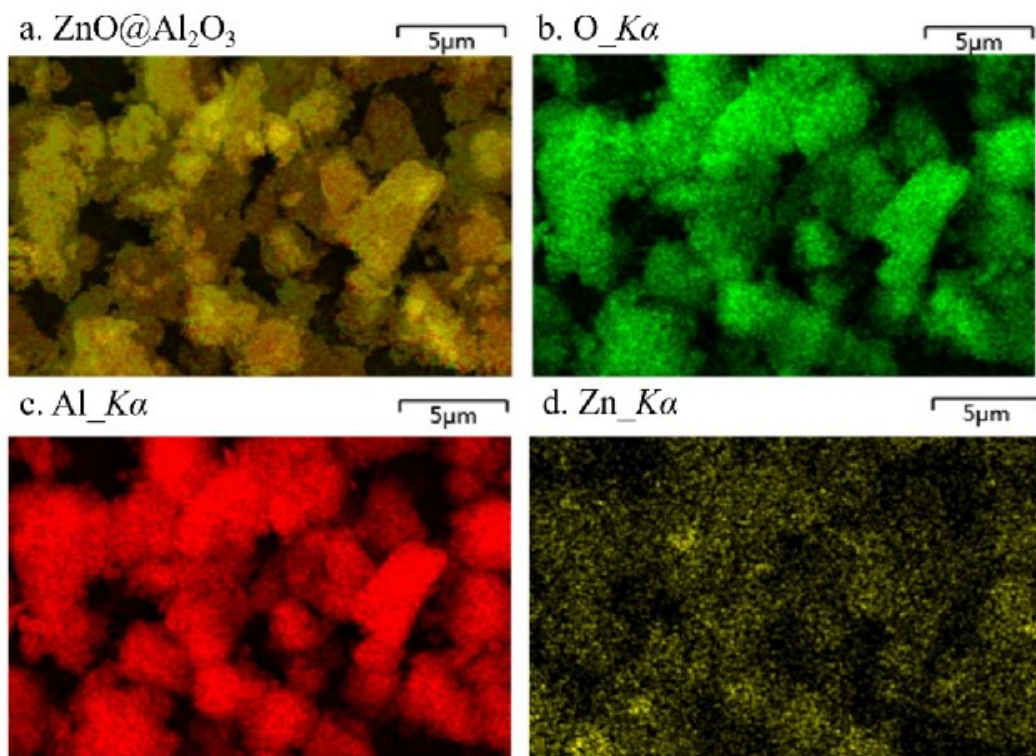


Figure S2 (a.) EDS X-ray mappings of ZnO@Al₂O₃ particles: (b.) O; (c.) Al and (d.) Zn maps, where the K α peak of the elements was used for the mapping.

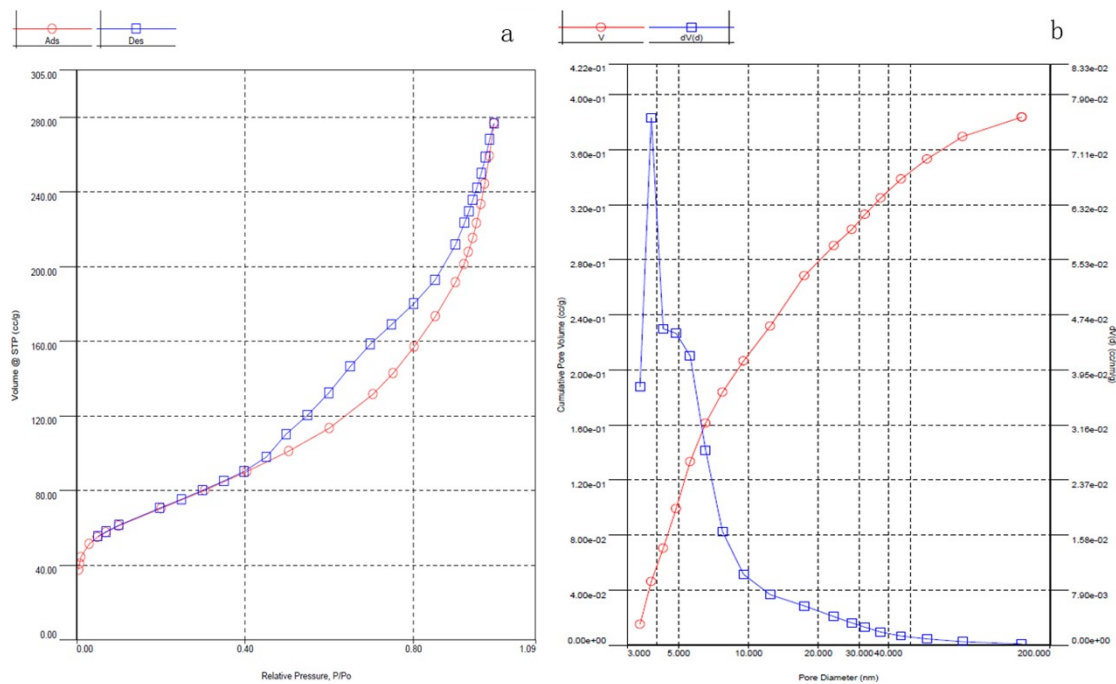


Figure S3 N₂ isotherm adsorption desorption curves of ZnO@Al₂O₃

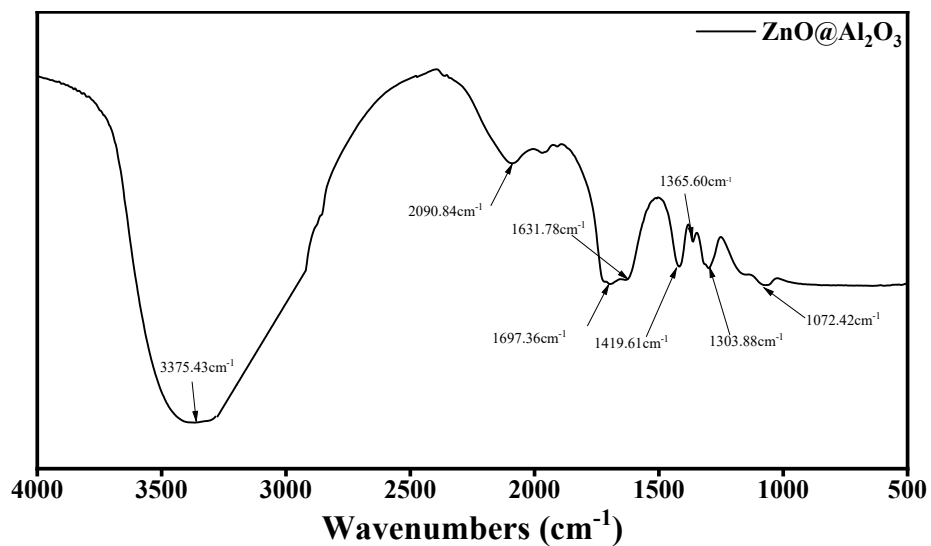


Figure S4 FTIR spectra of ZnO@Al₂O₃ particles

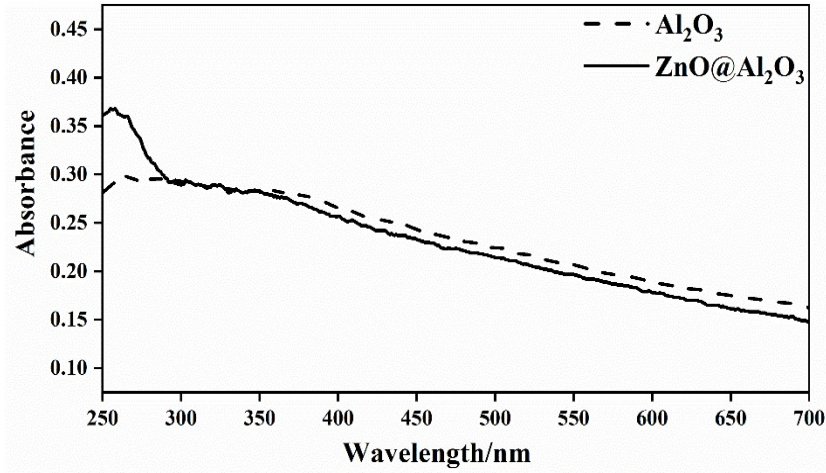


Figure S5 UV-VIS diffuse reflectance spectra of Al_2O_3 and $\text{ZnO@Al}_2\text{O}_3$

Text S2 Calculation of the ratios of gene abundance before and after experiments

The relative abundance of targeted genes could not be calculated precisely in terms of housekeeping genes since housekeeping genes possibly changed after disinfection or photoreactivation, thus the ratios of each gene abundance before and after experiments were calculated via Eq. (1) - Eq. (5) (Livak et al., 2001):

$$Y = X \times (1 + Ev)^{C_T} \quad (1)$$

$$\lg X = \log Y - C_T \times \lg(1 + Ev) \quad (2)$$

$$\lg X_1 - \lg X_2 = -C_{T1} \times \lg(1 + Ev) + C_{T2} \times \lg(1 + Ev) \quad (3)$$

$$\lg \frac{X_1}{X_2} = (C_{T2} - C_{T1}) \times \lg(1 + Ev) \quad (4)$$

$$\frac{X_1}{X_2} = 10^{(C_{T2} - C_{T1})} = (1 + Ev)^{-(C_{T1} - C_{T2})} \quad (5)$$

where Y was the number of amplifications, X was the number of initial DNA template, Ev was the amplification efficiency, C_T was the cycle threshold. Eq. (1) and Eq. (2) were the basic theory on qPCR. When two different number of initial DNA templates reached the same fluorescence threshold, the difference between $\lg X_1$ and $\lg X_2$ was gained by Eq. (3). Finally, the ratio of X_1 and X_2 was obtained in Eq. (5).

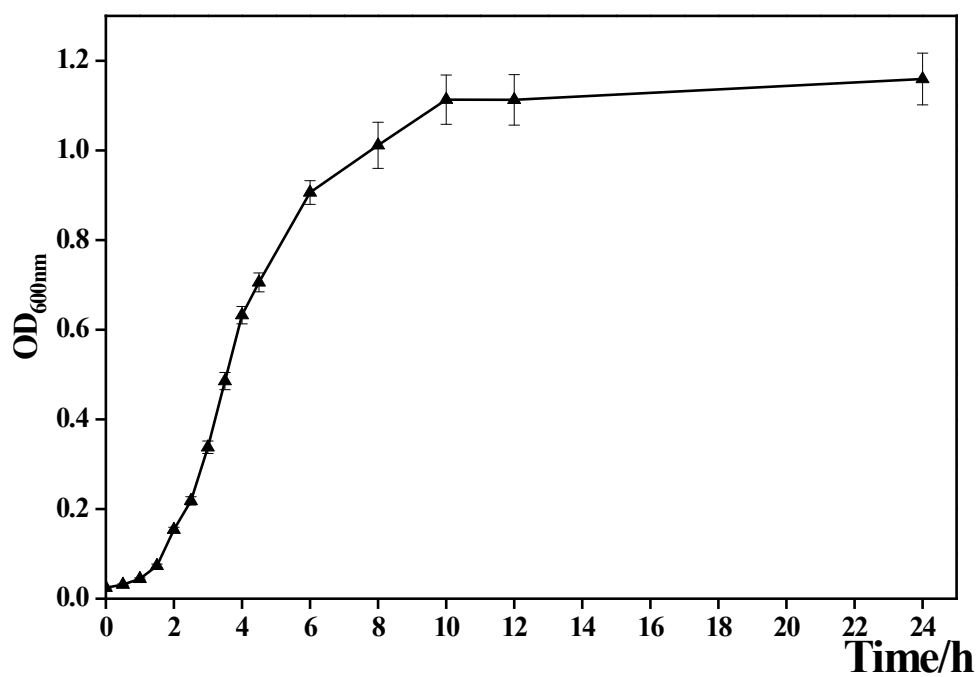


Figure S6 Growth curves of RP4-*E. coli* in selective liquid LB medium



Figure S7 Reactor for disinfection and photoreactivation

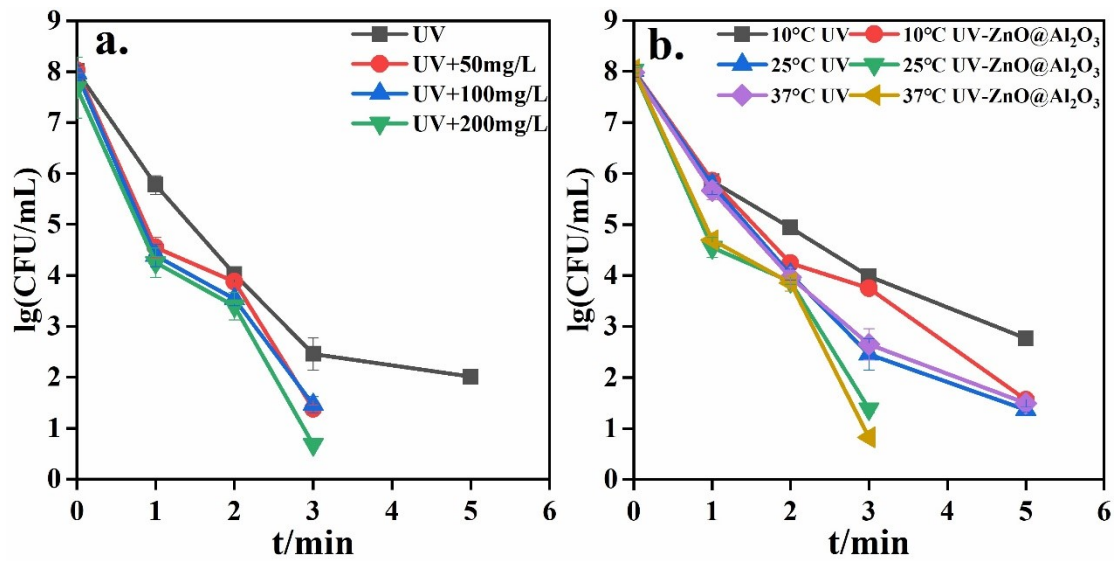


Figure S8 Survival numbers of RP4-*E. coli* in disinfection experiments over UV time.

a. T = 25 °C, [ZnO@Al₂O₃] = 0, 50, 100 and 200 mg/L; b. [ZnO@Al₂O₃] = 50 mg/L, T= 10, 25 and 37 °C

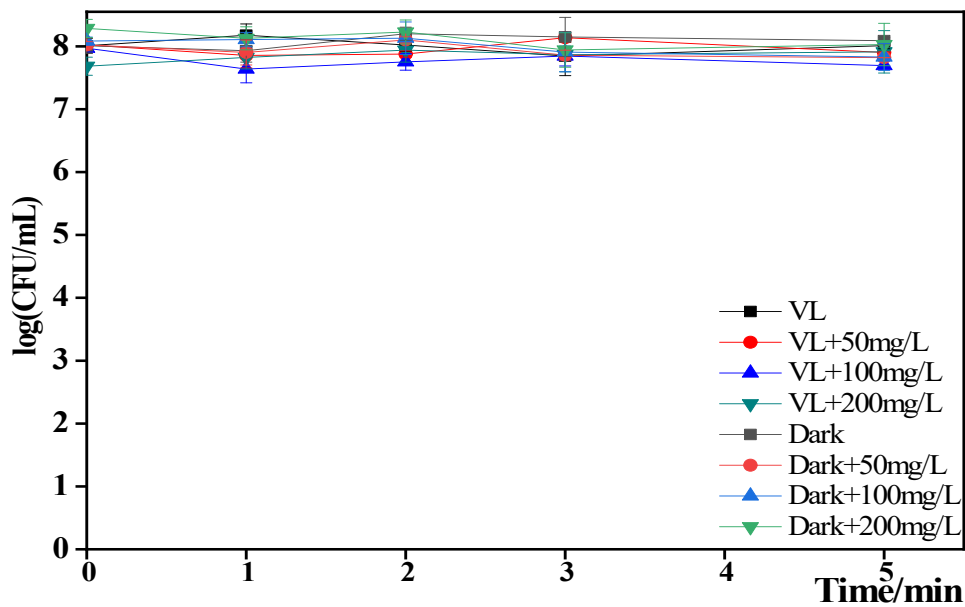


Figure S9 Bacterial numbers in absence and existence of ZnO@Al₂O₃ when bacteria were exposed to dark or VL

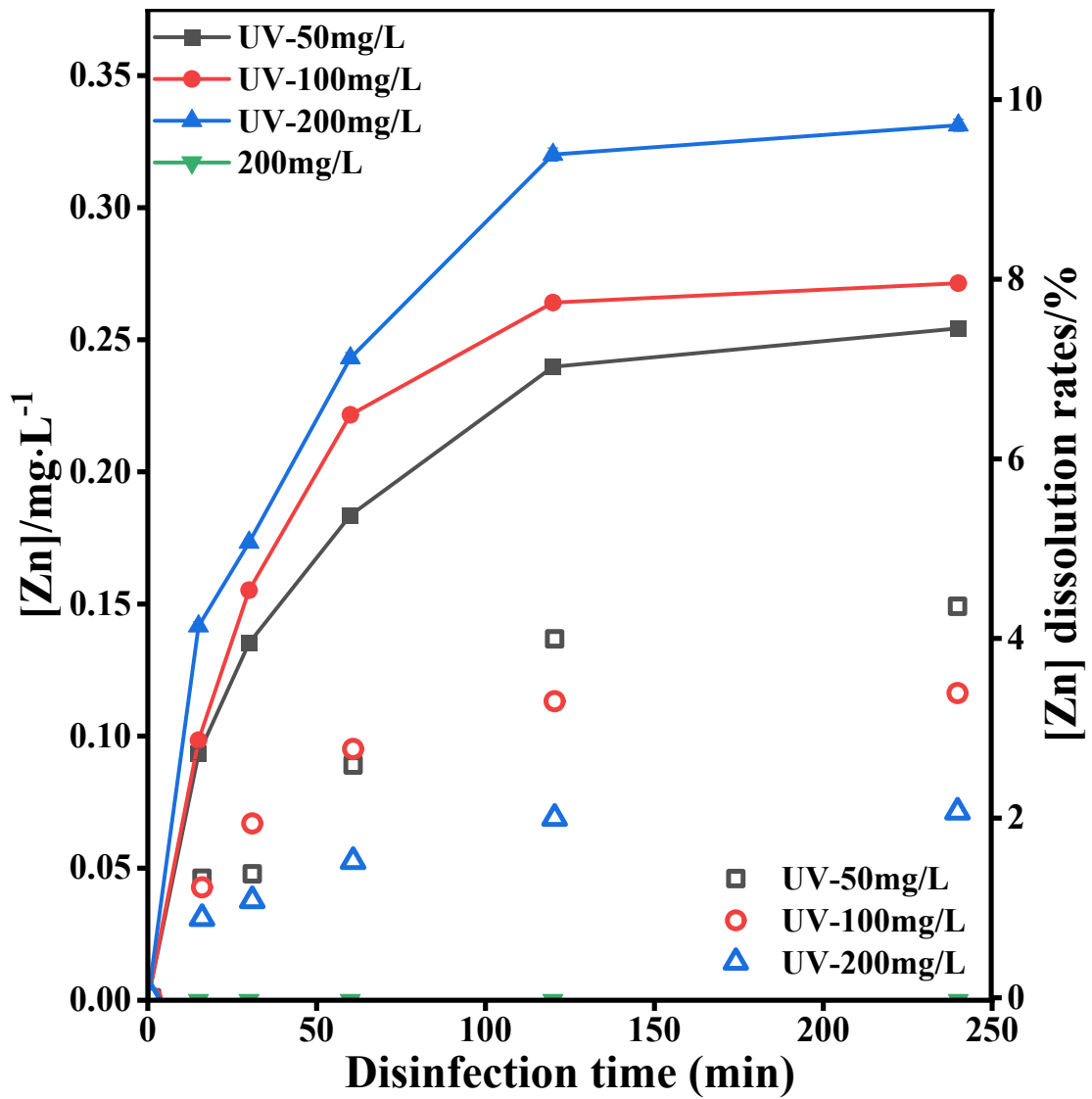


Figure S10 Zinc ion concentrations (left y) and dissolution rates (right y) over disinfecting time

(pH=7.0, T=25°C, target bacterial=RP4-*E. coli*)

Table S 1 Experimental conditions of photoreactivation

	Disinfection temperature/°C	ZnO@Al ₂ O ₃ dosage/mg·L ⁻¹	UV time/min	VL time/min
Changes in disinfection temperature and dosage	10	0	15	0、5、10、20、40、 60、120、180、240
		50		
		100		
		200		
	25	0		
		50		
		100		
		200		
	37	0		
		50		
		100		
		200		
Changes in UV time	25	0	15、30、60、	240
		50	120、240	
		100		
		200		

Table S 2 Sequences of primers for qPCR

Species	Genes	Primer	5`-3`	Length of Product	Source
MGEs	<i>traF</i>	<i>traF</i> -F	AAGTGTTTCAGGGTGCTTCTGC	118bp	[1]
		<i>traF</i> -R	GTCGCCTTAACCGTGGTGTT		
	<i>korA</i>	<i>korA</i> -F	TCGGGCAAGTTCTTGTCC	147bp	[1]
		<i>korA</i> -R	GCAGCAGACCATCGAGATA		
ARGs	<i>aphA</i>	<i>aphA</i> -F	CGACGGTAGAGCAAAGGT	198bp	[2]
		<i>aphA</i> -R	AGCGGACAGCATCAGTAA		
	<i>blaTEM-1</i>	<i>blaTEM-1</i> -F	CCAATGCTTAATCAGTGAGG	858bp	[3]
		<i>blaTEM-1</i> -R	ATGAGTATTCAACATTTCCG		
	<i>tetA</i>	<i>tetA</i> -F	GCTACATCCTGCTTGCCTTC	659bp	[4]
		<i>tetA</i> -R	CATAGATCGCCGTGAAGAGG		

[1] Zhang Y., Aprü Z. G., He M., et al. Subinhibitory Concentrations of Disinfectants Promote the Horizontal Transfer of Multidrug Resistance Genes within and across Genera. *Environmental Science & Technology*, 2017, 51(1):570.

[2] Xu L., Zhao J., Liu Z.M., Wang Z.Y., Yu K.Q., Xing B.S. Cleavage and transformation inhibition of extracellular antibiotic resistance genes by graphene oxides with different lateral sizes. *Science of the Total Environment*, 2019, 695, 133932.

[3] Domínguez-Pérez R. A., Rocio T. L., Mariana A. C., et al. Detection of the antibiotic resistance genes *blaTem-1*, *cfxA*, *tetQ*, *tetM*, *tetW*, and *ermC* in endodontic infections of a Mexican population. *Journal of Global Antimicrobial Resistance*, 2018, 15:20-24.

[4] Wang S., Xue N., Li W., et al. Selectively Enrichment of antibiotics and ARGs by microplastics in river, estuary and marine waters. *Science of The Total Environment*, 2019, 708:134594.